Synergy-Based Gaussian Process Estimation of Ankle Angle and Torque: Conceptualization for High Level Controlling of Active Robotic Foot Prostheses/ Orthoses

Mahdy Eslamy
Advanced Service Robots (ASR) Laboratory,
Department of Mechatronics Engineering,
Faculty of New Sciences and Technologies,
University of Tehran,
P.O. Box 1439957131,
Tehran 1439957131, Iran

Khalil Alipour[1]
Advanced Service Robots (ASR) Laboratory,
Department of Mechatronics Engineering,
Faculty of New Sciences and Technologies,
University of Tehran,
P.O. Box 1439957131,
Tehran 1439957131, Iran
e-mail: k.alipour@ut.ac.ir

Human gait is the result of a complex and fascinating cooperation between different joints and segments in the lower extremity. This study aims at investigating the existence of this cooperation or the so-called synergy between the shank motion and the ankle motion. One potential use of this synergy is to develop the high level controllers for active foot prostheses/orthoses. The central point in this paper is to develop a high level controller that is able to continuously map shank kinematics (inputs) to ankle angles and torques (outputs). At the same time, it does not require speed determination, gait percent identification, switching rules, and look-up tables. Furthermore, having those targets in mind, an important part of this study is to determine which input type is required to achieve such targets. This should be fulfilled through using minimum number of inputs. To do this, the Gaussian process (GP) regression has been used to estimate the ankle angles and torques for 11 subjects at three walking speeds (0.5, 1, and 1.5 m/s) based on the shank angular velocity and angle. The results show that it is possible to estimate ankle motion based on the shank motion. It was found that the estimation achieved less quality with only shank angular velocity or angle, whereas the aggregated angular velocity and angle resulted in much higher output estimation quality. In addition, the estimation quality was acceptable for the speeds that there was a training procedure before and when it was tested for the untrained speeds, the estimation quality was not as acceptable as before. The pros and cons of the proposed method are investigated at different scenarios.
[DOI: 10.1115/1.4041767]

1 Introduction

Human gait is the outcome of a complex and fascinating interaction between leg joints, brain, spinal cord, peripheral nerves, muscles, and bones. Humans elaborately exploit and take advantage of this unique neuro-musculo-skeletal structure to achieve their desired ambulation. In this regard, the intersegmental cooperation or the so-called synergy is a key component to achieve a specific stable locomotion [1]. Amputation is one main reason that creates disruption in this necessary cooperation.

For trans-tibial amputees, passive[2], semi-active[3], or active[4,5] foot prostheses are three different options that are currently available. The active ones might be more appealing, because potentially they can emulate the ankle kinematics and kinetics for different ambulation types and terrain surfaces and are capable to provide net positive power [2–5]. Unfortunately, such characteristics are missing in passive and semi-active ones [6].

To bring the potentials of these active devices into full reality, however, a number of challenges both in hardware and software domains should be resolved. One of the main challenges regarding the software, is to design the high level controller. A high level controller is in charge of estimating the current locomotion status of the user and accordingly commands the machine (i.e., the active prosthetic foot) to operate in line with the amputee user. It has been shown that the level and the rate of the human adaptation to the active foot prostheses can be related to the control method [7]. In that work, two control schemes (proportional myoelectric control and forefoot foot-switch control) were used to activate an artificial pneumatic muscle. The conclusion was that the proportional myoelectric control results in larger reductions in muscle activation and more similarity to normal gait kinematics in comparison to the foot-switch control.

To tackle the control challenge, a number of methods have been proposed by the research community. Those methods could be categorized into different groups. From one viewpoint, the methods could be divided to the discrete methods which require switching rules and the continuous methods. In Refs. [8] and [9], a single stride is divided into different sections (state-machines) based on the ankle kinematics and kinetics, and the motor (actuator) desired operation is determined accordingly based on if-then decision-making stations. In contrast, in Ref. [10] no division within a single stride is considered, and the motor status is determined continuously (seamlessly) within a step. This is achieved through the phase plane concept. Nevertheless, in order to determine the speed (or stride length) the high level controller uses if-then decision makings, and then, it continuously determines the desired motor positions within the stride based on a look-up table that is saved offline.

[1]Corresponding author.
Manuscript received March 26, 2018; final manuscript received September 27, 2018; published online November 29, 2018. Assoc. Editor: Guy M. Genin.
[2]https://www.ossur.com/prosthetic-solutions/products/balance-solutions/flex-foot-assure
[3]https://www.ossur.com/prosthetic-solutions/products/dynamic-solutions/pro prio-foot
[4]https://www.ottobock.com/en/press/press-releases/bionx.html
[5]https://springactive.com

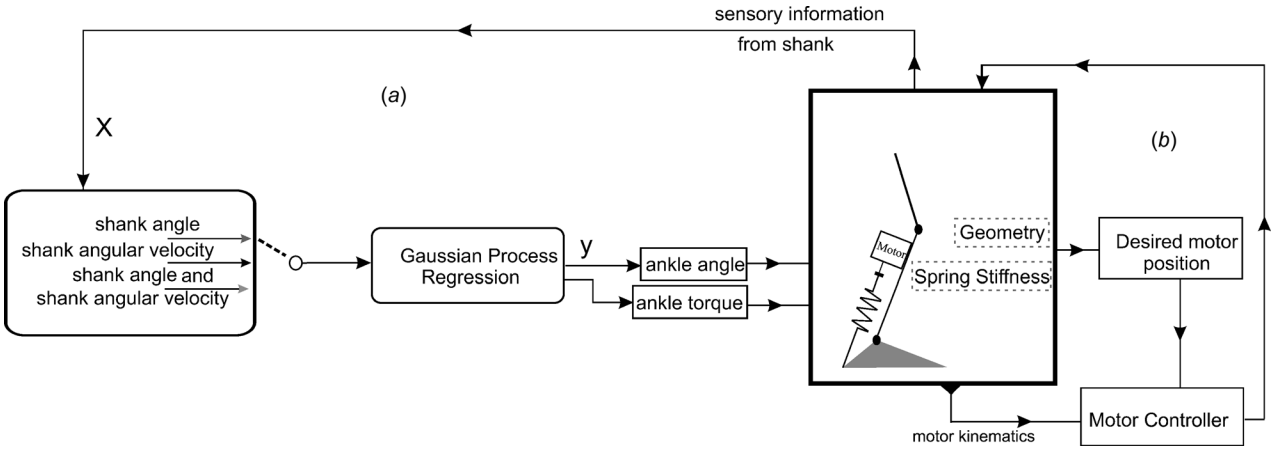

Fig. 1 The overall control structure for an active foot prosthesis. A part of the acquired sensory information (*X*) is used by the high level controller (section *a*) to estimate ankle angles and torques (or through the geometry of the active foot prosthesis and the spring stiffness, the desired motor positions are estimated). Furthermore, some part of the sensory data (e.g., motor position and/or velocity) is used to create the required command signal through the motor controller (section *b*) to actuate it. Note that different actuation mechanisms could be used for the active foot prostheses [23,24].

From the viewpoint of the type and number of the sensory information used to control active foot prostheses, the myoelectric electromyography (EMG) signals [11–13] and the mechanical sensors (ankle, foot or shank kinematics and kinetics) [8,10,14–20] are the most in use. In Ref. [21], it is shown that sensor fusion approach (EMG + mechanical) can result in better prosthesis control compared to the methods that use only EMG signals or only the mechanical sensors. The nonlinear autoregressive neural network with exogenous input was developed in Ref. [22] to continuously map within-socket EMG activity to prosthetic ankle angle in the sagittal plane. The model consisted of an input layer containing the windowed low frequency plantar- and dorsiflexor EMG signals recorded from the residual limb and ankle angle fed back from the model output [23,24].

Another important aspect of the high level controller is how to process the acquired sensory information. Support Vector Machines [21], Gaussian Mixture Models [14,25], Linear Discriminant Analysis [26,27], Neural Networks [26], Dynamic Bayesian Networks [28], and k-nearest neighbor [29] are the methods that have been used to process the sensory inputs and estimate the desired actuator (motor) status as output. The extended Kalman filter was used in Ref. [30] to estimate the prosthetic foot orientation with respect to the ground. This was achieved through two gyros and four infrared sensors (to measure distance of the foot from the ground). In echo method [31,32], the trajectories of the intact limb were estimated for the amputated side taking into account the required time delay between the motions of the two sides. Complementary limb motion estimation [33] uses principal component analysis to extract couplings between limbs in healthy side and then estimates the motion of the patient's affected limbs. Unlike echo-control, where the reference was a delayed replay of the sound leg's motion, in complementary limb motion estimation, states are mapped instantaneously.

As it is observed, different input types (either from mechanical or EMG sensors) were used for those proposed high level controllers. However, on the output side, usually the produced angles and torques and how close they are to the expected values, are under surveillance.

The fundamental point in this paper is to develop a high level controller for active foot prostheses that continuously maps (estimates) the inputs to the outputs, which at the same time, does not require switching rules, speed determination, gait percent identification, and look-up tables. Furthermore, having those targets in mind, an important part of this study is to determine which input type is required to achieve such targets. This should be fulfilled through using minimum number of inputs.

The reason to set such a goal is that the state-machine approaches are less appealing if a continuous approach could be planned which removes the need to think about those switching rules. In addition, the state-machine approach requires defining the angle-torque threshold values that determine the switching between the states. Therefore, the designer is required to define those rules and thresholds in a way that this method can be used for different locomotion types. Furthermore, study [10] showed that it is possible to have continuous approach toward designing the high level controllers. However, to do that, it was required to prepare and manipulate the input data (e.g., to add and multiply by some values based on a trial and error procedure), determine the speed and then the gait percent and finally determine the angle or torque values (or equivalently motor positions in their work) according to a look-up table.

To achieve the above-mentioned goals, we have used the strength of the Gaussian process (GP) regression [34]. GP creates (finds) relationship between the inputs and outputs based on the probability theory. In fact, it is a generalization of the Gaussian probability distribution [34]. GP is a nonparametric supervised machine learning approach which yields a distribution over all possible functions that satisfy the input–output relationship [34], the mean of which (f) could be used for estimation and prediction. In Ref. [35], GP was used for continuous prediction of the status of the missing limbs from intact limbs for a hand neuroprosthesis. GP has also been used to predict trajectories for the joint motions [36], where the training inputs were 12 body parameters which estimated the angles of hip, knee, and ankle joints (as outputs). In Ref. [37], GP regression was even used to predict the skin temperature due to the use of lower limb prostheses.

The paper structure is organized as follows. First, we explain the definitions, required information and the fundamentals and describe the viewpoint used in this study. Next, a string of different scenarios are planned, and the results are investigated for each scenario. At the end, we discuss different aspects and make final conclusions.

2 Method

2.1 Fundamentals and Basic Definitions. Figure 1 presents an overall view of the control scheme of the active foot prostheses. As seen, it is divided to two main sections. Section (a) is the high level controller and is responsible to estimate the ankle angles and torques corresponding to the current locomotion status of the subject. Section (b) is the motor controller, which could be,

Table 1 Subjects' information used in this study (mean ± standard deviation)

Number of subjects	Age (yr)	Body height (m)	Body mass (kg)	Speeds (m/s)
21	25.4 ± 2.7	1.73 ± 0.09	70.9 ± 11.7	Walking: 0.5, 1, 1.5

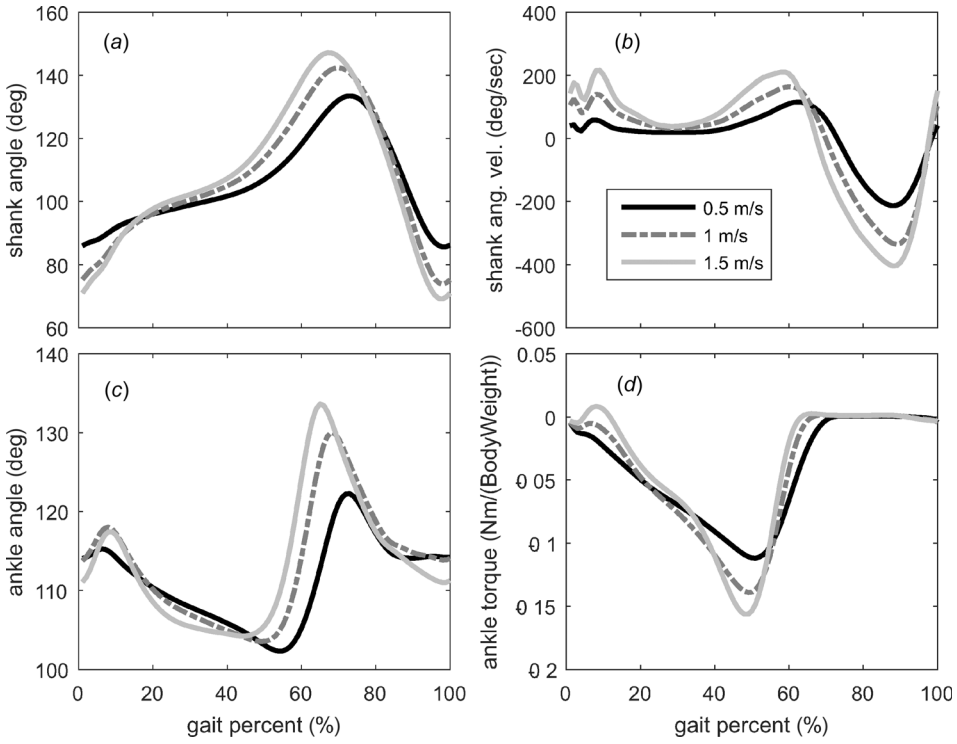

Fig. 2 The diagrams of (*a*) shank angle (θ_{sh}), (*b*) shank angular velocity ($\dot{\theta}_{sh}$), (*c*) ankle angle θ_a, and (*d*) ankle torque (T_a in [Nm/(BodyWeight)]) for 0.5, 1 and 1.5 m/s walking. The graphs are the mean of 21 subjects for each speed [38].

e.g., a proportional–derivative controller or an impedance controller (when interaction with environmental forces are also taken into account). Within the motor controller, the error signal is one important part and is formed using the actual sensor values (e.g., motor positions) and that provided desired value from the high level controller. The error is further processed using gains to finally create a command signal for the actuator (the motor) [38].

In this paper, the problem of developing a high level controller is converted into the problem of finding an appropriate function f that can acceptably map the inputs x into the outputs y. In other words, the aim is to investigate the existence of synergy between the motion of the shank as input x and ankle angles and torques as the outputs y. Based on a functional point of view, this can be stated as $y = f(x)$.

The shank-related inputs are its angular velocity $\dot{\theta}_{sh}$ and angle θ_{sh}. Therefore, $x = \dot{\theta}_{sh}$ or $x = \theta_{sh}$ depending on which input is under investigation. In addition, it is possible to make a combined input as $x = [\dot{\theta}_{sh}, \theta_{sh}]$. The effect of each input on the estimation of y will be investigated in Sec. 3. The shank angle is the angle between the horizontal line that passes through the knee and the shank itself. The outputs are ankle angles $y = \theta_a$ and ankle torques $y = T_a$ separately. The ankle angle is the angle between the human shank and the line that passes through the fifth metatarsal joint and the ankle joint (malleolus) [39].

The required data set has been obtained from 21 healthy subjects [39] in laboratory environment using motion capture cameras (Qualisys, Gothenburg, Sweden) and instrumented treadmill (type ADAL-WR, HEF Tecmachine, Andrezieux Boutheon, France). The general information about the subjects is given in Table 1. For each subject and speed at least 21 walking cycles were used to obtain mean data [39]. The walking direction was to the horizontal x direction. The subjects will be divided to training and testing groups as will be explained in Sec. 2.2. The data are related to walking 0.5, 1, 1.5 m/s (Table 1). In Fig. 2, the graphs for inputs ($\dot{\theta}_{sh}$ and θ_{sh}) and outputs ($y = \theta_a$ and $y = T_a$) are shown for those walking speeds.

In human biomechanics, the gait cycle starts with the heel contact and ends with the next contact of the same foot. A gait cycle is divided to one hundred sections called gait percent [40]. Each gait percent (at each speed) has its corresponding shank angular velocity, shank angle, ankle angle, and ankle torque as seen in Fig. 2. The start of the gait cycle (heel contact) was determined when the vertical ground reaction force exceeded 20 N [39].

2.2 The Gaussian Process Regression. To define f, the GP regression [34] has been used. A GP is defined by its mean $m(x)$ and covariance function $k(x, x')$ (for the input pair x and x') as [34]

$$f(x) \sim \mathcal{GP}(m(x), k(x, x')) \tag{1}$$

where $m(x) = E[f(x)]$ (E denotes expectation of $f(x)$) and $k(x, x') = E[(f(x) - m(x))(f(x') - m(x'))]$ [34]. To use GP for prediction, some priori trainings are required. The training inputs are in the form of $x = [\dot{\theta}_{sh}]$ or $x = [\theta_{sh}]$ or $x = [\dot{\theta}_{sh}, \theta_{sh}]$ depending on which input type is used and can be formed as $D = \{(x_i, f_i) | i = 1, \ldots, n\}$, where index i shows each (input) item out of one hundred items in case one speed is under investigation. Consequently, for three speeds, it would be three hundred items (remember that a gait cycle is divided to 100 sections called gait percent [40]). Therefore, $i = 1$ refers to the first gait percent of the first speed (0.5 m/s),

$i = 101$ refers to the first gait percent of the second speed (1 m/s) and $i = 201$ refers to the first gait percent of the third speed (1.5 m/s). Therefore, D consists of n observations, where x_i is a d-dimensional row vector (depending on whether one type of input is used $[\dot{\theta}_{sh}]$ or $[\theta_{sh}]$, or, two types $[\dot{\theta}_{sh}, \theta_{sh}]$), and f_i is the corresponding function (output) value. The effect of each input type is discussed in detail in Sec. 3. In addition, concatenating the training observations would form the aggregated input matrix X as

$$X = \begin{pmatrix} x_1 \\ x_2 \\ x_3 \\ \vdots \\ x_n \end{pmatrix}, \quad y = f = \begin{pmatrix} y_1 \\ y_2 \\ y_3 \\ \vdots \\ y_n \end{pmatrix} \tag{2}$$

To evaluate the performance of GP in terms of the prediction, a test set is also required. The test inputs are denoted with x^*. Accordingly, the outputs related to x^* are marked with f^* (or in fact $y^* = f^*(x^*)$).

It is logical to think that inputs close to each other would have quite similar output values and, therefore, train inputs that are close to the test inputs should be logically informative for prediction [34]. In GP, the covariance function k defines such a similarity. The covariance function is also a designer-defined parameter. GP benefits from several various covariance functions [34].[6] As an example, we examined the output quality using squared exponential function [34].[6] In another trial, the quality was examined when Matérn covariance function [34][6] was used. The Matérn class of covariance function is

$$k_{\text{Matérn}}(r) = \frac{2^{1-\nu}}{\Gamma(\nu)} \left(\frac{\sqrt{2\nu} r}{l} \right)^{\nu} K_{\nu} \left(\frac{\sqrt{2\nu} r}{l} \right) \tag{3}$$

r is the absolute difference of input pairs x and x' ($r = |x - x'|$), ν and l are positive parameters called hyperparameters Θ, where K_ν is a modified Bessel function, and Γ is the gamma function [34]. It was observed that the results related to the Matérn covariance function outperformed in comparison to other covariance functions (full list in Ref. [34])[6] including squared exponential function. One reason is that the squared exponential function is a special case of the Matérn covariance function when $\nu \to \infty$ [34]. One common approach to determine the hyperparameters Θ is to maximize the log marginal likelihood [34][6]

$$\log p(y|X, \Theta) = -\frac{1}{2} \left(y^T K(X,X) y + \log |K(X,X)| + n \log 2\pi \right) \tag{4}$$

in which $p(A|B)$ means conditional probability of A given that event B is true [34][6]. The first term of Eq. (4) addresses data fit, the second term introduces a complexity penalty and the last term is a normalization constant [34].[6] The log marginal likelihood automatically performs a trade-off between model fit and complexity. Several optimization algorithms exist for this purpose [34].[6] In this study, hyperparameters were optimized through exact inference method together with Gaussian likelihood, since the best output quality was observed through using these inference and likelihood methods. The inference method determines how to infer the posterior process, find hyperparameters, evaluate the log marginal likelihood, and make predictions.[6]

The joint distribution of the training outputs f and the test outputs f^* would be [34]

$$\begin{bmatrix} f \\ f^* \end{bmatrix} \sim \mathcal{N} \left(0, \begin{bmatrix} K(X,X) & K(X,X^*) \\ K(X^*,X) & K(X^*,X^*) \end{bmatrix} \right) \tag{5}$$

where $K(X, X^*)$ is the $n \times n^*$ matrix of the covariances evaluated at all pairs of training and test points. A $K(X, X)$ is defined as

$$K(X,X) = \begin{pmatrix} k(x_1,x_1) & k(x_1,x_2) & \cdots & k(x_1,x_n) \\ k(x_2,x_1) & k(x_2,x_2) & \cdots & k(x_2,x_n) \\ \vdots & \vdots & \vdots & \vdots \\ k(x_n,x_1) & k(x_n,x_2) & \cdots & k(x_n,x_n) \end{pmatrix} \tag{6}$$

A similar statement could be expected for other $K(.,.)$. $\mathcal{N}$ denotes normal distribution.

In light of Eq. (5), it is possible to obtain information for f^* on the condition of having X, f, and X^* as [34]

$$f^*|X, f, X^* \sim \mathcal{N}(\bar{f^*}, \text{cov}(f^*)) \tag{7a}$$

where

$$\bar{f^*} = K(X^*,X) K(X,X)^{-1} f \tag{7b}$$

$$\text{cov}(f^*) = K(X^*,X^*) - K(X^*,X) K(X,X)^{-1} K(X,X^*) \tag{7c}$$

where $\bar{f^*}$ and cov(f^*) are GP posterior mean and GP posterior covariance, respectively. Equation (7) provide the solution for f^* to estimate the desired outputs related to the unseen new inputs (i.e., the test inputs X^*) [34]. The result of the GP-based approach for defining f and the corresponding estimations will be investigated in detail for different subjects and speeds in Sec. 3.

For the training inputs/outputs, the mean shank/ankle data of ten randomly selected subjects were used. This has been done for each speed. The test inputs/outputs are related to each remaining individual subject (i.e., the remaining 11 subjects). For each subject, the mean data for a specific speed was used as test inputs to evaluate the estimation quality for that subject and that speed.

Intersubject testing procedure that is adopted in this study (i.e., the test subjects are different from the training subjects) will show the possibility of the generalization of our proposed method. Basically, it means that by having the shank data of any new subject, the method would estimate the ankle angles and torques for that speed. The intersubject testing was also used, e.g., in Refs. [41–43].

To evaluate the prediction quality, we use the root-mean-square (RMS) errors $\sqrt{\sum (y_{est} - y_{exp})^2 / n}$ (n is the number of samples which is 100 for each speed, y_{est} and y_{exp} are the estimated and the expected values for ankle angles or torques, respectively), the maximum (absolute) error and the commonly used R^2 values. These measures were also employed in different studies, e.g., see Refs. [41] and [44].

The RMS errors give information about the nature of the distribution of the estimated values around the curve for the expected ones. Following that, the maximum (absolute) errors give understanding about how far those deviations were with respect to the expected values. At the end, R^2 values give information about how close is the curve of the estimated values to the curve of the expected values. RMS errors and maximum errors equal to 0 and R^2 values equal to 1 would be the ideal values. Note that it is possible to have similar R^2 values with different RMS and maximum error values. Therefore, these separate pieces of information are provided to give a more comprehensive understanding about the nature of the estimations.

Note that there is no gold standard to define which estimation quality should be deemed as "acceptable" and which one as "not acceptable." However, in order to have a tool to draw conclusions about the impact of this study, we use the criterion that was used in Ref. [44] for the acceptable estimation quality. In that study, R^2 values higher than 0.8 were a sign of acceptable estimations (ideal is 1). Therefore, we will also use that definition to define whether estimation qualities are acceptable or not. Therefore, in Table 2, R^2 values less than 0.8 (unacceptable) are underlined and denoted by a cross. This facilitates a better visualization of the results.

[6] http://www.gaussianprocess.org/gpml

Table 2 R^2 values for different subjects and speeds (related to Sect. 3.2 (double-input scenario))

	Gait type →	Walking					
	Output →	Ankle angle θ_a (deg)			Ankle torque T_a (N·m)		
Subject number ↓	Speed (m/s) →	0.5	1	1.5	0.5	1	1.5
11		0.93	0.96	0.99	0.82	0.95	0.99
12		0.82	0.85	0.86	0.96	0.99	0.95
13		0.84	0.86	0.89	$\underline{0.74}^{\times}$	0.85	0.95
14		0.88	0.94	0.94	$\underline{0.79}^{\times}$	0.91	0.88
15		0.84	0.93	0.95	$\underline{0.83}$	0.88	0.95
16		$\underline{0.51}^{\times}$	0.86	0.85	0.88	0.97	0.99
17		$\underline{0.80}$	0.80	0.87	0.94	0.94	0.83
18		$\underline{0.64}^{\times}$	0.87	0.97	0.84	0.97	0.98
19		$\underline{0.91}$	0.88	0.83	$\underline{0.79}^{\times}$	0.89	0.94
20		0.93	0.97	0.96	$\underline{0.98}$	0.99	0.98
21		0.90	0.85	$\underline{0.76}^{\times}$	0.84	0.95	0.93
Mean		0.82	0.89	$\underline{0.90}$	0.86	0.94	0.94

Note: R^2 values less than 0.8 are underlined and denoted by a cross.

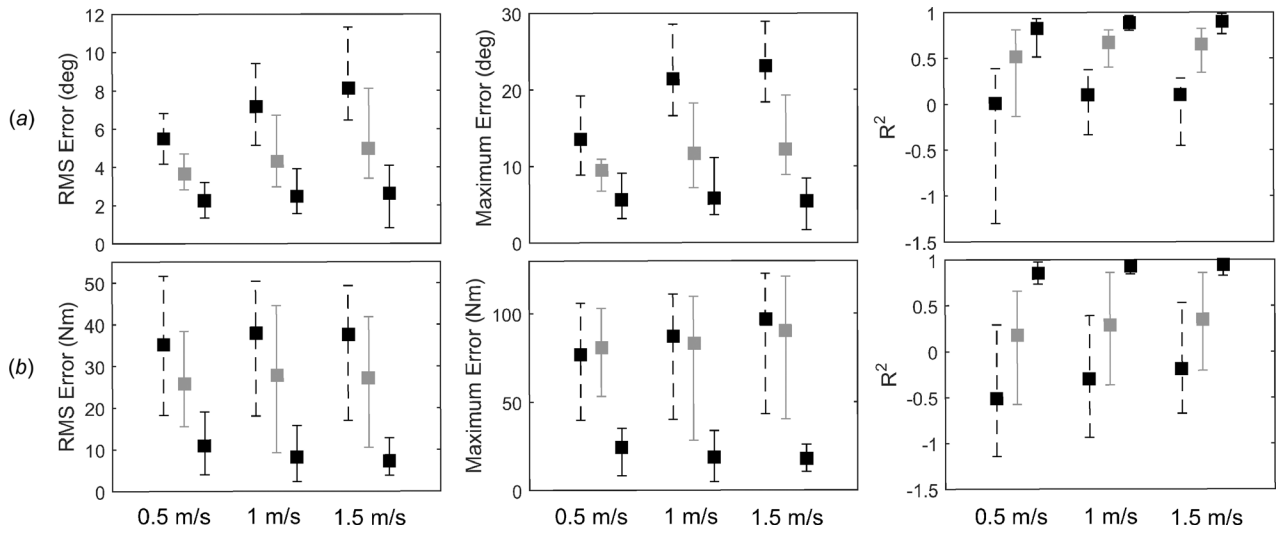

Fig. 3 (related to Sects. 3.1 and 3.2) (*a*) Related to ankle angle and (*b*) related to ankle torque. For each speed, the dotted black lines and squares are related to training with $\dot{\theta}_{sh}$, the gray solid lines and squares are related to training with θ_{sh} and the solid black lines and squares are related to training with $[\dot{\theta}_{sh}, \theta_{sh}]$. The squares show the mean (of the eleven test subjects) and the lower and upper bounds show the minimum and maximum for each parameter for walking 0.5, 1, 1.5 m/s.

3 Results

In Sec. 2, the GP provided the required tool to develop a continuous mapping from the inputs to the outputs without the need for speed determination, gait percent identification, look-up tables, and switching rules. Now, it is time to determine which input type results in the best estimation quality for this tool. The following scenarios clarify the answer to this issue.

At first, we evaluate the estimation quality with minimum number of inputs, i.e., input is only the shank angular velocities or the shank angles for each speed and subject.

3.1 Using Single-Input. In this scenario, the training and test inputs are the shank angular velocities $x = \dot{\theta}_{sh}$ and shank angles $x = \theta_{sh}$ separately. The inputs are related to 0.5, 1, and 1.5 m/s walking speeds. For each speed, the estimation results (mean, maximum and minimum of RMS errors, maximum absolute errors, and R^2 values) of the test group are shown for ankle angles and torques in Figs. 3(*a*) and 3(*b*). As it is seen, the results for single-input scenarios are not acceptable. One finding is that the estimation quality is more acceptable when the training input is θ_{sh}.

As observed, the single-input scenario has a poor estimation quality. One explanation for this observation is the relationship between the shank angular velocity or shank angle and ankle angle or torque. This has been shown in Fig. 4. As it is seen, for each shank angular velocity or angle (Figs. 4(*a*) and 4(*b*), (at least) two values of ankle angles can be found. This has the potential to create difficulties to estimate the acceptable output for a specific input. A similar relationship was also observed for ankle torques (the figure has not been shown). In contrast, as seen in Fig. 4(*c*), the number of the points that have the same $[\dot{\theta}_{sh}, \theta_{sh}]$ values but with different ankle angles, have declined considerably. Therefore, it is expected that the estimation quality in double-input scenario be more acceptable than the single-input scenarios. This matter will be investigated in Sec. 3.2.

As observed, in single-input scenarios the output quality was not acceptable. This motivated us to expand the investigations to double-input scenarios, where both shank angular velocities and angles are the inputs.

3.2 Using Double-Inputs $[\dot{\theta}_{sh}, \theta_{sh}]$. In this approach, the training and test inputs are the shank angular velocities and angles simultaneously as $x = [\dot{\theta}_{sh}, \theta_{sh}]$. The inputs are related to 0.5, 1,

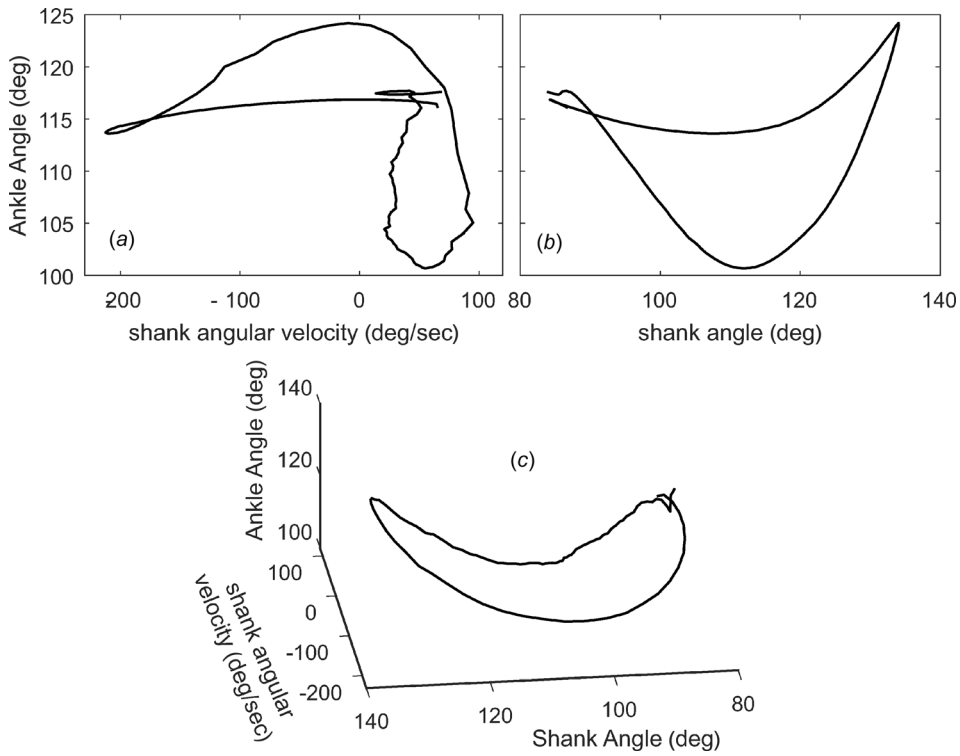

Fig. 4 (related to Sect. 3.1) The diagrams of ankle angle with respect to (*a*) $\dot{\theta}_{sh}$, (*b*) [θ_{sh}], and (*c*) [$\dot{\theta}_{sh}, \theta_{sh}$] (diagrams for speed of 0.5 m/s, subject number 11)

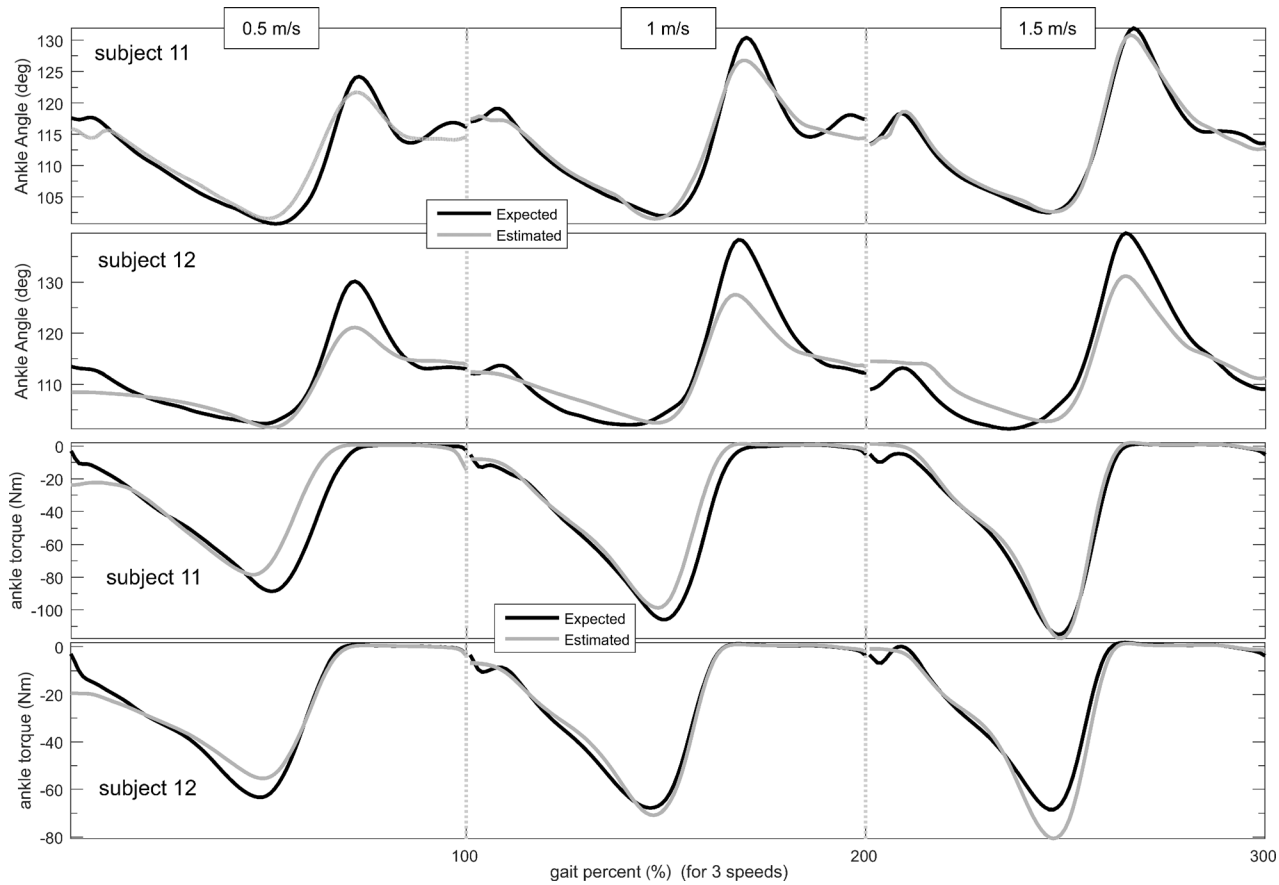

Fig. 5 (related to Sect. 3.2) The estimated and expected ankle angles and torques for two different subjects, input: [$\dot{\theta}_{sh}, \theta_{sh}$], for three speeds from left to right: walking 0.5, 1, 1.5 m/s. See also Fig. 4 and Table 2.

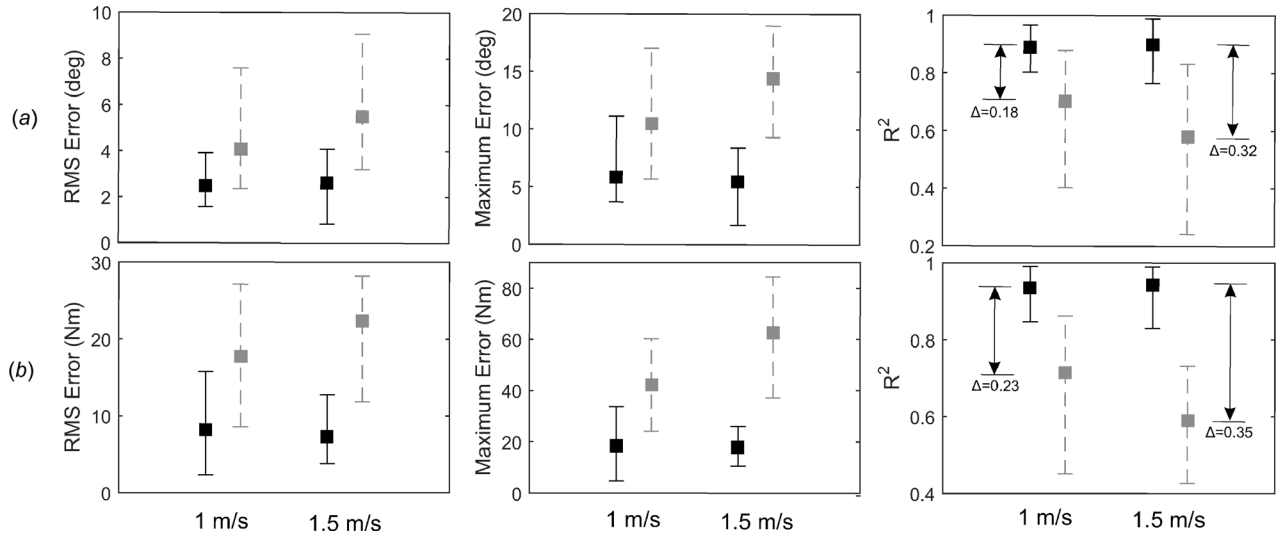

Fig. 6 (related to Sect. 3.3) (*a*) Related to ankle angle and (*b*) related to ankle torque, training with $[\dot{\theta}_{sh}, \theta_{sh}]$. For each speed, the solid black lines and squares are related to full training with data from 0.5, 1, and 1.5 m/s and the gray dotted lines and squares are related to training only with data from 0.5 m/s. For 1 and 1.5 m/s, the results for the untrained scenario are shown in comparison to the fully trained scenario. The squares show the mean (of the eleven test subjects) and the lower and upper bounds show the minimum and maximum for each parameter for walking 1 and 1.5 m/s.

and 1.5 m/s walking speeds as before. For each speed, the estimation results (mean, maximum, and minimum of RMS errors, maximum absolute errors and R^2 values) of the test group are shown for ankle angles and torques in Figs. 3(*a*) and 3(*b*). By this way, it is possible to evaluate the estimation quality in double-input scenario in comparison to the single-input approaches. Furthermore, for each test subject, the results for R^2 values are brought in Table 2 for each speed under investigations.

The results are brought in Table 2 for different individuals separately to give more comprehensive and subject-specific information and understanding about the nature of the estimations (the unacceptable R^2 values are underlined and denoted by a cross). As it is observed, out of 66 R^2 values, six values were not acceptable (9%) and 60 values were acceptable (91%). Furthermore, in Fig. 5, the estimated and expected ankle angles and torques are also shown for two test subjects.

As it is observed in Figs. 3(a) and (b), in double-input approach, the estimation qualities are much more acceptable than the results seen in Sec. 3.1 for the single-input approaches. In addition, the acceptance measures (RMS error, maximum error, and R^2 values) are highly correlated in this case ($p < 0.004, 0.002, 0.006$ for those three speeds, respectively).

3.3 Further Investigations. One of the questions that might arise is that if it is possible to estimate the ankle angles and torques for all three speeds by training the GP with (input data from) fewer number of speeds. To investigate this matter, GP was trained with input data ($[\dot{\theta}_{sh}, \theta_{sh}]$) only from 0.5 m/s (mean of those ten randomly selected subjects). Then, the estimation quality was tested for 0.5, 1 and 1.5 m/s (in other words, in this case, for 1 and 1.5 m/s, the high level controller was tested without previous training).

In Figs. 6(*a*) and 6(*b*), the results of the angle/torque estimations for the case in which the GP received full training for 0.5, 1, and 1.5 m/s are shown in comparison to the case without training for 1 and 1.5 m/s. As it is seen, the GP performance declined for those two untrained speeds. This is visible for all RMS errors, maximum errors, and R^2 values. It is also seen that the distance (Δ) between the mean of R^2 values (trained versus untrained) were higher in 1.5 m/s than 1 m/s (for angle and torque).

We continued this investigation and tested GP for the case it was trained for only 1 m/s and 1.5 m/s separately. The obtained results showed that the estimation based on the input data from only one speed could give acceptable results for that specific speed. However, for untrained speeds (i.e., the speeds for which there was no training process), the estimation quality declined in comparison to the case there was a previous training. This trend was observed for different subjects.

Next, the estimation quality was examined when GP was trained with the (input) data from two speeds (different combinations could be possible here for each subject). Similar to previous investigations, for a specific untrained speed, the estimation quality was less acceptable than the case there was a training.

As seen, in general, GP did not perform very acceptably in terms of extrapolation for untrained speeds. This can have different reasons. One reason is that GP is a supervised machine learning approach [34]. Therefore, it should not be very surprising why it did not perform well for extrapolation. Another reason might be that the number of the inputs was not enough. We used the shank angular velocity and angle. The results might change if we had included data for acceleration or other measurements. The other reason might be the type of the employed inputs. For example, a fusion of those kinematic inputs and, e.g., acceleration data or EMG signals might have better results in this regard. This requires more investigations in the future studies.

4 Discussions, Conclusions, and Suggestions

One of the questions that might come to mind is that we have used laboratory data set from motion capture cameras and what would happen if we used body-attached inertial measurement units (IMUs), since, in the latter, the sensory information is noisy. In case of using IMUs, usually filtering is required to have more smoothed data; however, after smoothing, the obtained data are quite similar to that of obtained from the laboratory motion capturing devices [10,45]. However, it should be noted that they are never identical, and there are always some differences which are inevitable due to the nature of the hardwares. A recent study [46] has shown that there was acceptable similarity between joint angles obtained from IMUs and the ones obtained from motion capture systems.

In this study, we developed a high level controller that estimated the ankle angle and torque (as outputs) based on shank angular velocity and angle (as inputs). This was achieved through using the existing synergy (the co-ordination and the cooperation) between the shank motion and the foot motion. The proposed

controller was continuously mapping the inputs to the outputs, did not require speed determination, gait percent identification, look-up tables, or switching rules. In this perspective, we showed that it is possible to remove the need for those requirements to develop the high level controllers for active foot prostheses (at least for walking gait). These characteristics are of high interest. However, at the same time, we showed that even in this approach there are some limitations. For example, in case of untrained speeds, we showed that the performance of the controller would decline.

The findings of this study can be used in the field of active prosthetics and orthotics. In design of such devices, an important issue is how to design the high level controller. The high level controller is in charge to provide the estimations of the ankle angle and torque so that the motor operation can be accordingly adjusted and finally can result in an appropriate locomotion in line with the users' expectations.

Two important factors in our proposed method were the tool required for such an approach and the nature of the inputs. We used Gaussian process as a tool and the shank motion as its input. Further studies could be made using other inputs. For example, shank linear or angular acceleration or EMG signals. The human locomotion is performed in a continuous manner. Based on this fact, we developed a continuous high level controller that removed the need for thinking and designing so many rules and state-machines, at least for a wide range of walking speeds.

One main advantage for this approach is that, in case of a transtibial amputee, the motion of the remaining part of the shank can be used in order to estimate the motion of the missing foot similar to Ref. [10] (although our approach was totally different as it was explained in detail in this study).

As the remaining limb's motion is governed by the user's Central Nervous System, its motion during walking can be used as a reliable input to the high level controller and the required estimations. This was already shown in Ref. [10]. In addition, for real world design, inertial measurement units could be embedded in an active foot prosthesis with little effort. In this case, the only required sensory information would be the shank angular velocity. The shank angle could be obtained via integration from the shank angular velocity. One important point in this case is the drift due to integration. In Ref. [45], we used a modified integrator to solve this problem. Note that in our proposed method in this study, we do not depend on the real physical meaning of the inputs. In our approach, the only important matter is that "if it is possible to establish acceptable relationship between the inputs and the outputs." We showed that it was possible. Our approach is different from the state-machine approaches, where real values of the ankle angles and torques are used to switch between the states.

The results show that the performance of the proposed high level controller was acceptable for different test subjects (see Table 2 for mean R^2 values). On the other side, the algorithm was sensitive to the "level of training" (see Figs. 6(*a*) and 6(*b*), section R^2), i.e., for a specific speed, you can expect acceptable results from the high level controller when you have trained it for.

The outputs of the high level controller are required as inputs to the low level controller. Depending on the design of the low level controller, these inputs could be further processed. If motor positions are directly controlled, then these inputs together with the prosthesis geometry and the spring stiffness are required to calculate the desired motor positions. If the torque is directly controlled, then the low level controller tries to follow the provided torque outputs from the high level controller. Basically, it depends on how the error is defined in the low level controller. Based on the error and the gains, the low level controller sends the required commands to the motor.

We are currently conducting parallel investigations in order to find out the pros and cons of the GP-based estimations from biomechanical point of view. In addition, we are investigating if this machine learning approach could be enhanced through combining with other techniques so that the estimations could be extended to other human gaits as well.

Acknowledgment

The experiments to obtain the required data for this work were conducted in Lauflabor Laboratory, Technical University of Darmstadt, Germany. The authors would like to thank the anonymous reviewers for their valuable comments and helpful suggestions to improve the quality of this paper.

Funding Data

- The Iranian Elites Foundation.

References

[1] Borghese, N. A., Bianchi, L., and Lacquaniti, F., 1996, "Kinematic Determinants of Human Locomotion," J. Physiol., **494**(3), pp. 863–879.

[2] Au, S. K., Weber, J., and Herr, H., 2009, "Powered Ankle-Foot Prosthesis Improves Walking Metabolic Economy," IEEE Trans. Rob., **25**(1), pp. 51–66.

[3] Hitt, J., Sugar, T., Holgate, M., Bellman, R., and Hollander, K., 2009, "Robotic Transtibial Prosthesis With Biomechanical Energy Regeneration," Ind. Rob. Int. J., **36**(5), pp. 441–447.

[4] Sup, F., Varol, H., Mitchell, J., Withrow, T., and Goldfarb, M., 2009, "Self-Contained Powered Knee and Ankle Prosthesis: Initial Evaluation on a Transfemoral Amputee," IEEE International Conference on Rehabilitation Robotics (ICORR), Kyoto, Japan, June 23–26, pp. 638–644.

[5] Cherelle, P., Matthys, A., Grosu, V., Vanderborght, B., and Lefeber, D., 2012, "The Amp-Foot 2.0: Mimicking Intact Ankle Behavior With a Powered Transtibial Prosthesis," Fourth IEEE RAS and EMBS Conference on Biomedical Robotics and Biomechatronics (BioRob), Rome, Italy, June 24–27, pp. 544–549.

[6] Postema, K., Hermens, H., De Vries, J., Koopman, H., and Eisma, W., 1997, "Energy Storage and Release of Prosthetic Feet—Part 1: Biomechanical Analysis Related to User Benefits," Prosthet. Orthot. Int., **21**(1), pp. 17–27.

[7] Cain, S. M., Gordon, K. E., and Ferris, D. P., 2007, "Locomotor Adaptation to a Powered Ankle-Foot Orthosis Depends on Control Method," J. Neuroeng. Rehabil., **4**(1), p. 48.

[8] Au, S., Berniker, M., and Herr, H., 2008, "Powered Ankle-Foot Prosthesis to Assist Level-Ground and Stair-Descent Gaits," Neural Networks, **21**(4), pp. 654–666.

[9] Sup, F., Varol, H. A., Mitchell, J., Withrow, T., and Goldfarb, M., 2008, "Design and Control of an Active Electrical Knee and Ankle Prosthesis," IEEE RAS & EMBS International Conference on Biomedical Robotics and Biomechatronics (BioRob), Scottsdale, AZ, Oct. 19–22, pp. 523–528.

[10] Holgate, M., Sugar, T., and Bohler, A., 2009, "A Novel Control Algorithm for Wearable Robotics Using Phase Plane Invariants," IEEE International Conference on Robotics and Automation (ICRA), Kobe, Japan, May 12–17, pp. 3845–3850.

[11] Au, S., Bonato, P., and Herr, H., 2005, "An EMG-Position Controlled System for an Active Ankle-Foot Prosthesis: An Initial Experimental Study," IEEE International Conference on Rehabilitation Robotics (ICORR), Chicago, IL, June 28–July 1, pp. 375–379.

[12] Ferris, D. P., Gordon, K. E., Sawicki, G. S., and Peethambaran, A., 2006, "An Improved Powered Ankle–Foot Orthosis Using Proportional Myoelectric Control," Gait Posture, **23**(4), pp. 425–428.

[13] Koller, J. R., Remy, C. D., and Ferris, D. P., 2017, "Comparing Neural Control and Mechanically Intrinsic Control of Powered Ankle Exoskeletons," IEEE International Conference on Rehabilitation Robotics (ICORR), London, July 17–20, pp. 294–299.

[14] Varol, H., Sup, F., and Goldfarb, M., 2010, "Multiclass Real-Time Intent Recognition of a Powered Lower Limb Prosthesis," IEEE Trans. Biomed. Eng., **57**(3), pp. 542–551.

[15] Varol, H., Sup, F., and Goldfarb, M., 2009, "Powered Sit-to-Stand and Assistive Stand-to-Sit Framework for a Powered Transfemoral Prosthesis," IEEE International Conference on Rehabilitation Robotics, (ICORR), Kyoto, Japan, June 23–26, pp. 645–651.

[16] Varol, H., Sup, F., and Goldfarb, M., 2009, "Real-Time Gait Mode Intent Recognition of a Powered Knee and Ankle Prosthesis for Standing and Walking," IEEE RAS and EMBS International Conference on Biomedical Robotics and Biomechatronics (BioRob), Scottsdale, AZ, Oct. 19–22, pp. 66–72.

[17] Sup, F., Bohara, A., and Goldfarb, M., 2008, "Design and Control of a Powered Transfemoral Prosthesis," Int. J. Rob. Res., **27**(2), pp. 263–273.

[18] Eilenberg, M., Geyer, H., and Herr, H., 2010, "Control of a Powered Ankle–Foot Prosthesis Based on a Neuromuscular Model," IEEE Trans. Neural Syst. Rehabil. Eng., **18**(2), pp. 164–173.

[19] Hollander, K. W., and Sugar, T. G., 2007, "A Robust Control Concept for Robotic Ankle Gait Assistance," IEEE 10th International Conference on Rehabilitation Robotics, (ICORR), Noordwijk, The Netherlands, June 13–15, pp. 119–123.

[20] Oymagil, A. M., Hitt, J. K., Sugar, T., and Fleeger, J., 2007, "Control of a Regenerative Braking Powered Ankle Foot Orthosis," IEEE International Conference on Rehabilitation Robotics (ICORR), Noordwijk, The Netherlands, June 13–15, pp. 28–34.

[21] Huang, H., Zhang, F., Hargrove, L. J., Dou, Z., Rogers, D. R., and Englehart, K. B., 2011, "Continuous Locomotion-Mode Identification for Prosthetic Legs

Based on Neuromuscular–Mechanical Fusion," IEEE Trans. Biomed. Eng., **58**(10), pp. 2867–2875.
[22] Farmer, S., Silver-Thorn, B., Voglewede, P., and Beardsley, S. A., 2014, "Within-Socket Myoelectric Prediction of Continuous Ankle Kinematics for Control of a Powered Transtibial Prosthesis," J. Neural Eng., **11**(5), p. 056027.
[23] Grimmer, M., Eslamy, M., Gliech, S., and Seyfarth, A., 2012, "A Comparison of Parallel- and Series Elastic Elements in an Actuator for Mimicking Human Ankle Joint in Walking and Running," IEEE International Conference Robotics and Automation (ICRA), Saint Paul, MN, May 14–18, pp. 2463–2470.
[24] Eslamy, M., Grimmer, M., and Seyfarth, A., 2012, "Effects of Unidirectional Parallel Springs on Required Peak Power and Energy in Powered Prosthetic Ankles: Comparison Between Different Active Actuation Concepts," IEEE International Conference on Robotics and Biomimetics (ROBIO), Guangzhou, China, Dec. 11–14, pp. 2406–2412.
[25] Kilicarslan, A., Prasad, S., Grossman, R. G., and Contreras-Vidal, J. L., 2013, "High Accuracy Decoding of User Intentions Using EEG to Control a Lower-Body Exoskeleton," 35th Annual International Conference of the IEEE Engineering in Medicine and Biology Society (EMBC), Osaka, Japan, July 3–7, pp. 5606–5609.
[26] Huang, H., Kuiken, T., and Lipschutz, R., 2009, "A Strategy for Identifying Locomotion Modes Using Surface Electromyography," IEEE Trans. Biomed. Eng., **56**(1), pp. 65–73.
[27] Young, A. J., Simon, A. M., Fey, N. P., and Hargrove, L. J., 2013, "Classifying the Intent of Novel Users During Human Locomotion Using Powered Lower Limb Prostheses," International IEEE/EMBS Conference on Neural Engineering (NER), San Diego, CA, Nov. 6–8, pp. 311–314.
[28] Young, A. J., Simon, A. M., Fey, N. P., and Hargrove, L. J., 2014, "Intent Recognition in a Powered Lower Limb Prosthesis Using Time History Information," Ann. Biomed. Eng., **42**(3), pp. 631–641.
[29] Varol, H., and Goldfarb, M., 2007, "Real-Time Intent Recognition for a Powered Knee and Ankle Transfemoral Prosthesis," IEEE 10th International Conference on Rehabilitation Robotics (ICORR), Noordwijk, The Netherlands, June 13–15, pp. 16–23.
[30] Scandaroli, G. G., Borges, G. A., Ishihara, J. Y., Terra, M. H., da Rocha, A. F., and de Oliveira Nascimento, F. A., 2009, "Estimation of Foot Orientation With respect to Ground for an above Knee Robotic Prosthesis," IEEE/RSJ International Conference on Intelligent Robots and Systems (IROS), St. Louis, MO, Oct. 10–15, pp. 1112–1117.
[31] Grimes, D., Flowers, W., and Donath, M., 1977, "Feasibility of an Active Control Scheme for Above Knee Prostheses," ASME J. Biomech. Eng., **99**(4), pp. 215–221.
[32] Grimes, D. L., 1979, "An Active Multi-Mode Above Knee Prosthesis Controller," Ph.D. thesis, Massachusetts Institute of Technology, Cambridge, MA.
[33] Vallery, H., Van Asseldonk, E. H., Buss, M., and van der Kooij, H., 2009, "Reference Trajectory Generation for Rehabilitation Robots: Complementary Limb Motion Estimation," IEEE Trans. Neural Syst. Rehabil. Eng., **17**(1), pp. 23–30.
[34] Rasmussen, C. E., and Williams, C. K. I., 2006, *Gaussian Processes for Machine Learning*, The MIT Press, Cambridge, MA.
[35] Xiloyannis, M., Gavriel, C., Thomik, A. A., and Faisa, A. A., 2015, "Gaussian Process Regression for Accurate Prediction of Prosthetic Limb Movements From the Natural Kinematics of Intact Limbs," 7th International IEEE/EMBS Conference on Neural Engineering (NER), Montpellier, France, Apr. 22–24, pp. 659–662.
[36] Yun, Y., Kim, H.-C., Shin, S. Y., Lee, J., Deshpande, A. D., and Kim, C., 2014, "Statistical Method for Prediction of Gait Kinematics With Gaussian Process Regression," J. Biomech., **47**(1), pp. 186–192.
[37] Mathur, N., Glesk, I., and Buis, A., 2016, "Skin Temperature Prediction in Lower Limb Prostheses," IEEE J. Biomed. Health Inf., **20**(1), pp. 158–165.
[38] Ogata, K., 2002, *Modern Control Engineering*, 4th ed, Prentice Hall, Upper Saddle River, NJ.
[39] Lipfert, S., 2010, *Kinematic and Dynamic Similarities Between Walking and Running*, Verlag Dr. Kovac, Hamburg, Germany.
[40] Whittle, M. W., 2003, *Gait Analysis: An Introduction*. Butterworth-Heinemann, Oxford, UK.
[41] Goulermas, J., Howard, D., Nester, C., Jones, R., and Ren, L., 2005, "Regression Techniques for the Prediction of Lower Limb Kinematics," ASME J. Biomech. Eng., **127**(6), pp. 1020–1024.
[42] Findlow, A., Goulermas, J., Nester, C., Howard, D., and Kenney, L., 2008, "Predicting Lower Limb Joint Kinematics Using Wearable Motion Sensors," Gait Posture, **28**(1), pp. 120–126.
[43] Ardestani, M. M., Zhang, X., Wang, L., Lian, Q., Liu, Y., He, J., Li, D., and Jin, Z., 2014, "Human Lower Extremity Joint Moment Prediction: A Wavelet Neural Network Approach," Expert Syst. Appl., **41**(9), pp. 4422–4433.
[44] Bogey, R. A., and Barnes, L. A., 2017, "An EMG-to-Force Processing Approach for Estimating In Vivo Hip Muscle Forces in Normal Human Walking," IEEE Trans. Neural Syst. Rehabil. Eng., **25**(8), pp. 1172–1179.
[45] Eslamy, M., 2014, "Emulation of Ankle Function for Different Gaits Through Active Foot Prosthesis: Actuation Concepts, Control and Experiments," Ph.D. thesis, Technische Universität, Darmstadt, Germany.
[46] Al-Amri, M., Nicholas, K., Button, K., Sparkes, V., Sheeran, L., and Davies, J. L., 2018, "Inertial Measurement Units for Clinical Movement Analysis: Reliability and Concurrent Validity," Sensors, **18**(3), pp. 719–747.